

Refractive indices of human skin tissues at eight wavelengths and estimated dispersion relations between 300 and 1600 nm

Huafeng Ding¹, Jun Q Lu¹, William A Wooden², Peter J Kragel³ and Xin-Hua Hu¹

¹ Department of Physics, East Carolina University, Greenville, NC 27858, USA

² Department of Surgery, Brody School of Medicine, East Carolina University, Greenville, NC 27858, USA

³ Department of Pathology, Brody School of Medicine, East Carolina University, Greenville, NC 27858, USA

E-mail: hux@ecu.edu

Received 7 September 2005, in final form 3 January 2006

Published 1 March 2006

Online at stacks.iop.org/PMB/51/1479

Abstract

The refractive index of human skin tissues is an important parameter in characterizing the optical response of the skin. We extended a previously developed method of coherent reflectance curve measurement to determine the *in vitro* values of the complex refractive indices of epidermal and dermal tissues from fresh human skin samples at eight wavelengths between 325 and 1557 nm. Based on these results, dispersion relations of the real refractive index have been obtained and compared in the same spectral region.

(Some figures in this article are in colour only in the electronic version)

1. Introduction

Understanding the response of the skin to optical radiation is essential to the dermatological applications of photomedicine. Among various skin optical parameters, refractive index is an important one. At the microscopic scales ranging from 1 to 10 μm , refractive index variation causes light scattering which can be understood by direct solution of the Maxwell equations within the framework of classical electrodynamics for simple shaped particles (Bohren and Huffman 1983, Ma *et al* 2003a) and for biological cells (Lu *et al* 2005). For highly turbid tissues of human skin with sizes of 1 mm or larger, modelling of tissue optics based on the electrodynamic theory is very difficult, and the real refractive index and scattering parameters are often treated as independent parameters within the frameworks of effective medium theory and radiative transfer theory, respectively. For example, in the widely used method of Monte Carlo simulation of light distribution in biological tissues, photon interaction with an interface

between tissue regions of different refractive indices is described according to the Fresnel equations which require the index as the key parameter (van Gemert *et al* 1989, Wang *et al* 1995, Lu *et al* 2000). Furthermore, accurate modelling of measured light signals near a skin surface requires the refractive indices of skin tissues to account for the redistribution of light due to the index mismatch at the surface (Lu *et al* 2000, Meglinsky and Matcher 2001, Bartlett and Jiang 2001, Ma *et al* 2003b, 2005).

Determination of the refractive indices of the human skin tissues, however, presents challenges because of their highly turbid natures. In transparent or absorbing media such as the aqueous solutions with molecular solutes, propagation of light is dominated by its coherent component. The reflection and refraction of a light beam, as it passes through an interface between two media of different refractive indices, are described with the Fresnel equations on the basis of an effective medium theory. In contrast, light propagation in a turbid medium produces a scattering component that becomes increasingly dominant as the light penetrates into the medium. This feature of interaction often precludes the use of refraction method to determine the refractive index of biological tissue samples where uniform and thin samples are very difficult to obtain. Recently, we developed an automated reflectometer system for determining the refractive index of a turbid sample by measurement of its coherent reflectance R versus the incident angle θ without the need to section skin tissues (Ding *et al* 2005). Here we report complex refractive indices of fresh human skin tissues determined by nonlinear regression of $R(\theta)$ with the Fresnel equations. The complex refractive index has been obtained at eight wavelengths between 325 and 1557 nm for both the epidermis and dermis tissues. With these data we investigated various dispersion schemes for interpolation of the index data at other wavelengths in this spectral region.

2. Methods

Fresh skin tissue patches were obtained from the patients undergoing abdominoplasty procedures at the plastic surgery clinic of the Brody School of Medicine, East Carolina University (ECU). A study protocol approved by the Institutional Review Board of ECU was strictly followed and a consent form was signed by each participating patient before the surgery. We obtained one skin tissue patch from each of the 12 female patients with ages between 27 and 63 years old; 10 are Caucasian and 2 are African Americans, with the skin data compiled in table 1. Each skin patch was stored in a bucket on crushed ice ($\sim 2^\circ\text{C}$) inside a refrigerator immediately after surgery. Samples with sizes of about $1\text{ cm} \times 1\text{ cm}$ were prepared by removing the hair on the skin surface with scissors and subcutaneous fat tissue with a razor blade and warming the skin to a room temperature of about 22°C with 0.9% saline drops. Care was taken to preserve the stratum corneum layer of the skin epidermis. The skin sample was pressed against the base of the prism with a pistol pressurized by a nitrogen gas cylinder to maintain good contact between the sample and the prism. The periphery of the tissue sample between the pistol and prism base was sealed with plastic tape to prevent sample dehydration during the measurement. By pressing either the epidermis or dermis side of the skin sample against the prism base, the coherent reflectance curves of skin epidermis or dermis were measured, respectively. All reflectance curve measurements were performed at the room temperature within 30 h after the abdominoplasty procedure.

An automated reflectometer system has been designed and constructed to measure the coherent reflectance as a function of incident angle. Compared to other approaches of index determination based on fibre insertion and OCT (Bolin *et al* 1989, Tearney *et al* 1995, Knuttel and Boehlau-Godau 2000), this method has the combined benefits of high accuracy, wide spectral capability and instrumentation simplicity. The system has been described in detail

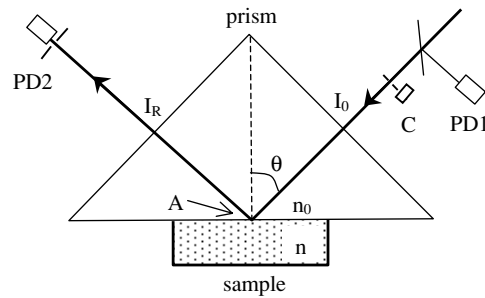


Figure 1. The schematic of the reflectometer system.

Table 1. The human skin sample data.

ID no.	Age	Race	Tissue location	Skin type	Measurement
1	42	Caucasian	Abdomen	III	Pressure dependence
2	40	Caucasian	Abdomen	I	633 nm, 532 nm
3	27	African American	Abdomen	V	442 nm
4	63	Caucasian	Abdomen	II	1064, 850 nm
5	56	Caucasian	Abdomen	II	325, 1550 nm
6	54	Caucasian	Arm	II	1310, 633 nm
7	34	Caucasian	Abdomen	II	1064, 325 nm
8 ^a	55	Caucasian	Abdomen	I	532, 633 nm
9 ^a	49	Caucasian	Abdomen	III	442, 1310 nm
10 ^a	41	Caucasian	Abdomen	II	850, 1550 nm
11 ^a	39	African American	Abdomen	V	532, diffuse reflection
12	44	Caucasian	Abdomen	III	Pressure dependence

^a The skin structures of the samples from these patients have been examined through histology.

elsewhere (Ding *et al* 2005). Briefly, a right-angle glass prism was used to interface with a skin sample on the prism base and a linear polarized laser beam was propagated through one side surface as the incident beam on the prism–sample interface at an incident angle of θ . The coherent reflectance R of the laser beam was measured at the angle of specular reflection by a photodiode of either Si or GaAs, depending on the light wavelength. Two coherent reflectance curves, $R_s(\theta)$ or $R_p(\theta)$, have actually been measured for each sample with either s- or p-polarized incident beam, respectively. The incident angle θ can be varied between 48° and 80° with a stepsize of 0.125° and resolution of 0.006° . A schematic diagram of the optical setup is presented in figure 1. The powers of the incident and reflected beams were measured by two identical photodiodes and the effect of the reflection loss at the side surfaces of the prism was removed to determine the coherent reflectance (R_s or R_p). To reduce the contribution of diffuse reflection to reflection signal, a pinhole of 2 mm diameter was used in front of the photodiode, resulting in an angular range of 1.74×10^{-2} rad or about 1.00° in the measurement. The incident laser beam, modulated at 370 Hz for lock-in detection, was produced by one of seven continuous-wave (cw) lasers at one of eight wavelengths: $\lambda = 325, 442, 532, 633, 850, 1064, 1310$ and 1557 nm. The diameter of the beam was set to between 1 and 2 mm with the incident beam power adjusted to be about $1 \mu\text{W}$.

The measured coherent reflectance curves have been fitted by the calculated values, $\tilde{R}_s(\theta)$ and $\tilde{R}_p(\theta)$, according to the Fresnel equations. The fitting requires the assumed value of the

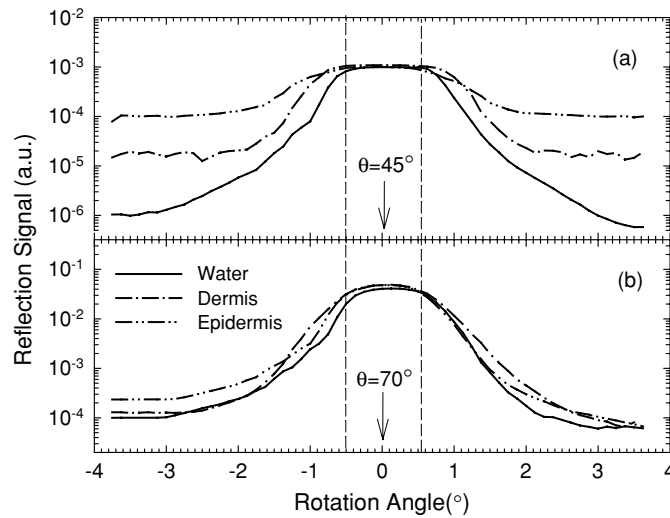


Figure 2. The reflection signal versus rotation angle of the detector at the incident angle of (a) $\theta = 45^\circ$; (b) $\theta = 70^\circ$ with a s-polarized beam at $\lambda = 633$ nm for deionized water, the epidermis and dermis of one skin sample. The error bars of about $\pm 5\%$ were removed for clear view and the two dashed lines indicate the angular acceptance range of the aperture in front of the photodiode.

complex refractive index of the turbid sample, $n = n_r + in_i$, and the known refractive index, n_0 , of the prism. Therefore, the index n was inversely determined using an iteration process to achieve least-squared difference between the calculated and measured curves (Ding *et al* 2005). The consistency between the measured and calculated coherent reflectance curves is described by a coefficient of determination, R^2 , defined as

$$R^2 = 1 - \frac{\sum_{i=1}^N (R_i - \tilde{R}_i)^2}{\sum_{i=1}^N (R_i - \bar{R})^2}, \quad (1)$$

where R_i and \tilde{R}_i denote the measured and calculated reflectances at the i th angle of incidence θ_i , respectively, and \bar{R} is the mean value of measured reflectance over N values of θ . The R^2 value ranges between 0 and 1 with $R^2 = 1$ for a perfect fit. The system was calibrated before measurements of each sample by comparing the measured real refractive index of deionized water with the published value at the wavelength of measurements (Hale and Query 1973). From the water data, the experimental error in determination of the real refractive index n_r of transparent samples by the reflectometer system was found to be about $\delta n_r = \pm 0.002$.

3. Results

To ensure that the reflection signal is dominated by its coherent component, we measured the angular distribution of the reflected beam around a specular reflection angle at two positions ($\theta = 45^\circ$ or 75°) with $\lambda = 633$ nm. Similar data with deionized water were used as the baseline and all are plotted in figure 2. These results demonstrate that the contribution of the diffusely reflected light to the coherent reflectance signal is negligible within the 1° angular range defined by the photodiode aperture (indicated by the dashed lines in figure 2). Two typical sets of coherent reflectance curves from the epidermis and dermis sides of the skin

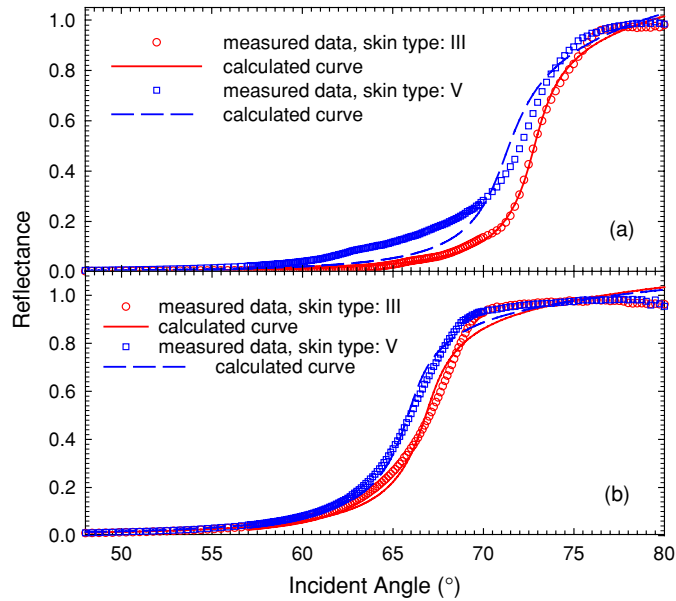


Figure 3. The typical measured coherent reflectance curves of two skin samples from two patients at $\lambda = 442$ nm with a s-polarized incident beam: (a) epidermis, (b) dermis. The solid lines are calculated curves based on the Fresnel equations with the following values of the complex refractive index: (a) $n = 1.445 + i1.00 \times 10^{-2}$ for ID no. 3 (skin type: V) and $n = 1.458 + i8.34 \times 10^{-3}$ for ID no. 9 (skin type: III); (b) $n = 1.394 + i9.30 \times 10^{-3}$ for ID no. 3 and $n = 1.404 + i9.20 \times 10^{-3}$ for ID no. 9.

samples of two patients with different skin types are presented in figure 3 together with the fitted curves based on the Fresnel equations. From these results one can see that the agreement between the measured and calculated reflectance curves varies from sample to sample and is gauged by the coefficient of determination R^2 . To determine the sensitivity of the refractive index on the nonlinear regression, we analysed the relation between R^2 and n with selected data of the coherent reflection curves and typical results are presented in figure 4. On the basis of the standard deviations in the distribution of R^2 values, we estimated that the uncertainty in obtaining the real and imaginary is about $\Delta n_r = \pm 0.006$ and $\Delta n_i = \pm 0.005$, respectively, for the turbid tissues of both the epidermis and dermis.

To select an appropriate pressure applied to the skin tissue sample for achieving good contact between the sample and prism with minimal tissue damage, we determined the complex refractive index from two skin samples as a function of the pressure, as shown in figure 5. It can be seen from the data that the real index is not sensitive to the air pressure set between 2×10^5 and 5×10^5 Pa. Signs of damage to the skin samples became visible when the pressure was increased to above 4×10^5 Pa, which included the fast dehydration of the tissue samples and significant reduction in the dermis layer thickness. On the basis of these results, all subsequent measurements of coherent reflectance of skin tissue samples were carried out at a fixed pressure of 2.06×10^5 Pa (30 psi or 2.0 atm) to minimize possible structural change in the skin tissues.

At each wavelength, 8 or 12 skin samples were used to measure the coherent reflectance curves of $R_s(\theta)$ and $R_p(\theta)$ with 4 from one patient. Half of the samples were measured with the epidermis side in contact with the prism base and half with the dermis side. The measurement of $R_s(\theta)$ and $R_p(\theta)$ was repeated three times on the same skin sample and thus the data set

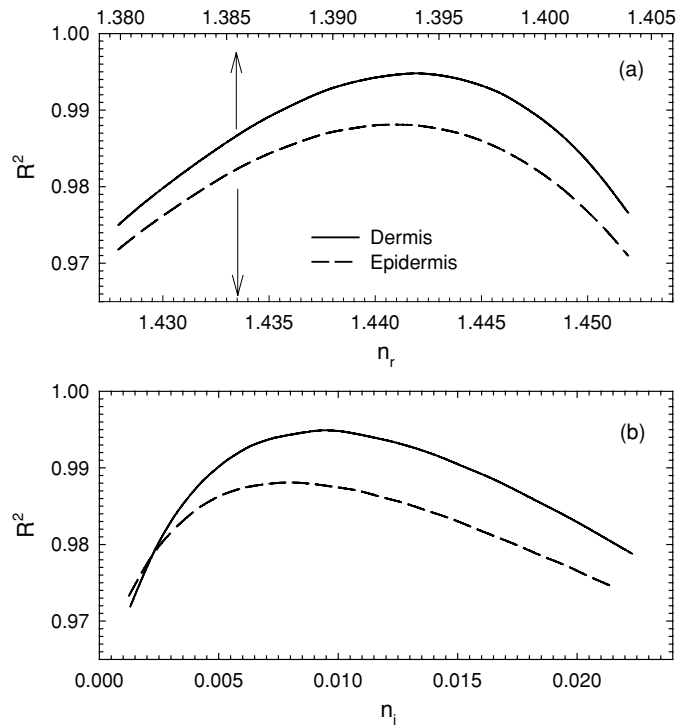


Figure 4. The dependence of the coefficient of determination R^2 on different choices of n_i for a coherent reflectance curve measured from the epidermis and dermis sides of a skin sample at $\lambda = 442$ nm.

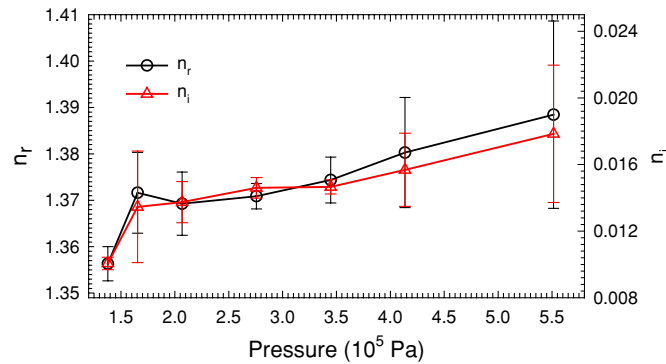


Figure 5. The average real and imaginary refractive index versus sample pressure determined from the dermis of two skin samples.

at each wavelength consists of 12 or 18 curves with an incident beam of s- or p-polarization. Nonlinear regression to the coherent reflectance curve data by the Fresnel equations was done individually to obtain the complex refractive index from each measurement. The coefficient of determination R^2 ranges from 0.960 to 0.999 for the data from the measurement of the epidermis side and from 0.978 to 0.998 for the dermis side. The mean values and standard deviations of the complex refractive index have been calculated at each wavelength from the

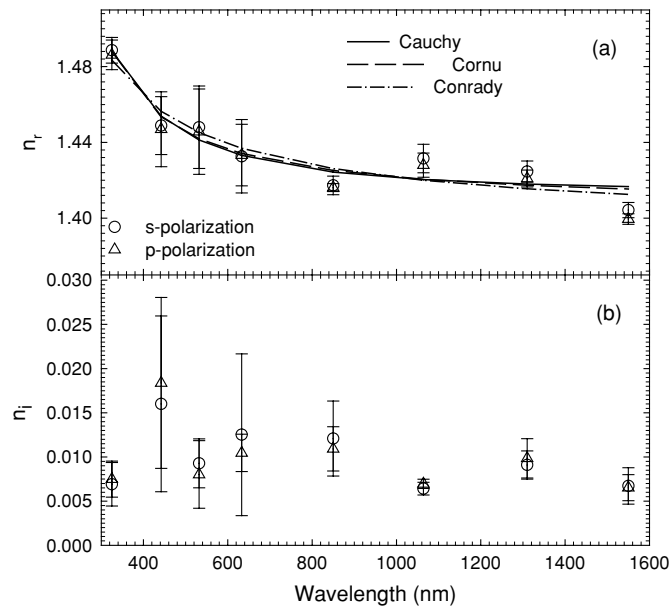


Figure 6. The (a) real and (b) imaginary refractive indices of human skin epidermis versus wavelength. Each data point and associated error bar is the mean and standard deviation obtained from 12 or 18 measurements of 4 or 6 skin samples. The lines in (a) are based on the dispersion equations.

data sets. These results are plotted as a function of wavelength in figure 6 for the epidermis and figure 7 for the dermis.

We investigated various dispersion schemes to identify appropriate ones for calculation of real refractive index of human skin tissues at wavelengths between 300 and 1600 nm based on our index data at eight wavelengths. Among those reported on the index data of ocular tissues (Kroger 1992, Atchison and Smith 2005), we selected three schemes to fit to our data: the Cauchy dispersion equation

$$n_r = A + \frac{B}{\lambda^2} + \frac{C}{\lambda^4}, \quad (2)$$

the Cornu equation

$$n_r = A + \frac{B}{(\lambda - C)} \quad (3)$$

and the Conrady equation

$$n_r = A + \frac{B}{\lambda} + \frac{C}{\lambda^{3.5}}. \quad (4)$$

The coefficients of each dispersion scheme determined with the least-squares principle from our index data are given in table 2.

4. Discussion

Refractive index plays an important role in characterization of the biological tissues' response to optical illumination, particularly for tissues of heterogeneous composition such as the layered skin tissues (Tuchin 2005). The real refractive index not only influences optical

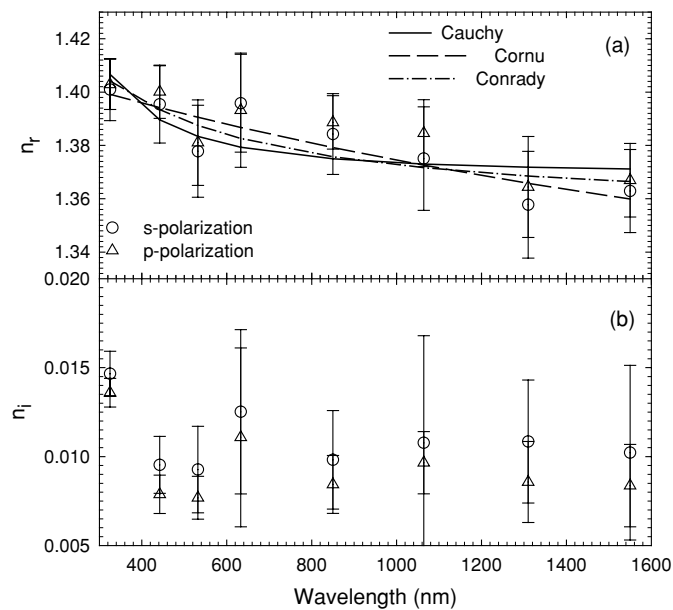


Figure 7. The (a) real and (b) imaginary refractive indices of human skin dermis versus wavelength. Each data point and associated error bar is the mean and standard deviation obtained from 12 or 18 measurements of 4 or 6 skin samples. The lines in (a) are based on the dispersion equations.

Table 2. The coefficients of different dispersion equations^a.

Dispersion equation	<i>A</i>	<i>B</i>	<i>C</i>
Cauchy	1.3696	3.9168×10^3	2.5588×10^3
Cornu	1.2573	4.5383×10^2	2.8745×10^3
Conrady	1.3549	1.7899×10	-3.5938×10^6

^a These coefficients were obtained on the basis of equations (2)–(4) with wavelength in the unit of nanometres.

pathlengths of light propagating in tissues that can be determined by the methods of phase or time-resolved spectroscopy (Duncan *et al* 1995, Zhao *et al* 2002) but also affects the light measurement outside the tissues due to the index mismatch at the boundaries (Meglinsky and Matcher 2001, Bartlett and Jiang 2001, Ma *et al* 2003b, 2005). With an automated reflectometer system, we have extended the technique of measuring the coherent reflectance curve (Meeten and North 1995, Ding *et al* 2005) to obtain the complex refractive indices of fresh human skin tissues. These results, therefore, are of interest to researchers wishing to conduct quantitative optical studies involving index-mismatched interfaces in the human skin.

The measurement of coherent reflectance was validated by confirming the dominance of the coherent reflection over the diffused one at the specular reflection angle for both of the epidermis and dermis sides of the skin samples, as shown in figure 2. Diffuse reflection occurs mainly outside the angular range defined by the aperture of the photodiode PD2 (see figure 1) and decreases towards the baseline data of water for large incident angles as θ approaches 80° . The diffusely reflected light originates from two sources: the rough tissue surface mismatched optically with the prism glass and the tissue bulk. From the index data

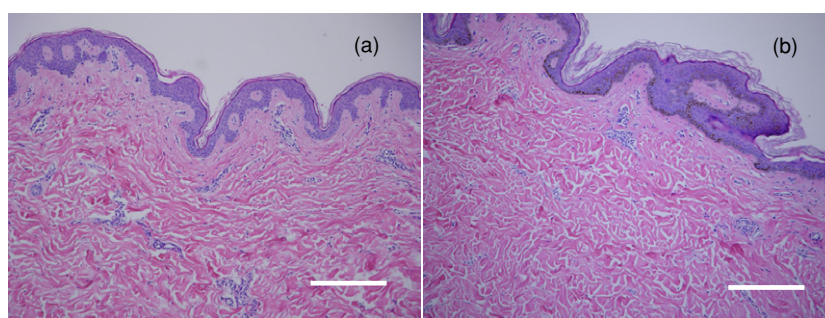


Figure 8. The microscope images of the histology slides of the skin samples from two patients: (a) ID no. 9 (skin type: III); (b) ID no. 11 (skin type: V). Bar = 100 μm .

presented in figures 6 and 7, we note that the index mismatch between the epidermis tissue and the BK7 glass of the prism is smaller than that of the dermis. Combining this fact with the knowledge of the skin epidermis having larger scattering coefficient than the dermis (van Gemert *et al* 1989), one can conclude that the diffuse reflection of the skin tissues seen in figure 2 should be dominated by the light scattering in the tissue bulk. This is consistent with our previous results on comparison of the diffuse reflection between the porcine skin tissues with rough surfaces and the intralipid solution samples with smooth surface (Ding *et al* 2005).

The human skin has a layered structure with two primary layers of epidermis and dermis, both are beneath the superficial layer of the epidermis or the stratum corneum (sc). We examined the tissue structures by preparing histological slides of the skin tissue samples from 4 patients (with ID no. from 8 to 11, see table 1) with standard H&E staining. Two examples of skin slides are shown in figure 8 with one from a Caucasian and another from an African American patient. It can be seen that the sc layer is less than 10 μm in thickness, as expected, with the thickness of epidermis ranging from about 30 to 80 μm . We further verified that the sc layer has no significant effect on the refractive index determination by comparing the index values from samples with and without the sc layer prepared from fresh porcine skin tissues. The sc layer was removed from the epidermal side of the porcine tissue samples using a tape-stripping method (Beisson *et al* 2001) without heating the samples. The real refractive index n_r of the epidermis at the wavelengths of 442 nm and 1064 nm was found to be the same within the experimental errors between the samples with and without the sc layer. These results demonstrated that the sc layer has no significant effect on the real refractive index of the skin epidermis because of its small thickness in comparison with the penetration depth (Everett *et al* 1966, van Gemert *et al* 1989), see also the discussion below. Another point worth noting is the effect of the melanin on the refractive index of the skin tissues. As can be seen from figure 8, many basal keratinocytes containing melanin pigment are visible near the epidermal–dermal junction in patient no. 11 (skin type: V), while little pigment exists in patient no. 9 (skin type III). The high density of melanin in the type V skins appears only to affect significantly the imaginary refractive index of epidermis, as shown in figure 3.

A general model of refractive index for a dense and turbid medium remains an open question. But according to the existing models of effective medium for absorbing or dilute turbid media (Ballenegger and Weber 1999, Barrera and Garcia-Valenzuela 2003) the refractive index determined from a coherent reflectance curve should relate to the medium's optical response from over at least the full depth of penetration of the coherent component of the incident wave in the medium. The total attenuation coefficients, as the sum of the scattering and absorption coefficients, for both the skin epidermis and dermis are expected to be on the

orders of 1 to 10 mm⁻¹ based on the published data (van Gemert *et al* 1989, Ma *et al* 2005) in the spectral region from 300 to 1600 nm. Consequently, the penetration depth for the coherent component should be about a few hundred micrometres or less. Therefore, one would expect the tissue response of the first 100 μm layer to dominate the coherent reflectance and thus the value of the real refractive index. This conclusion is supported by the wavelength correlation of the real refractive index determined from the epidermis and dermis sides of the skin tissue samples. The correlation coefficient of wavelength dependence of the real refractive index was found to be $r_{\text{corr}} = 0.99$ between the index determined with s- and p-polarized beam for the epidermis and $r_{\text{corr}} = 0.95$ for the dermis. The values of r_{corr} decrease drastically to 0.057 and 0.065 between the index of epidermis and dermis measured with the s- and p-polarized beam, respectively.

Within the previously discussed uncertainty on the real refractive index, our *in vitro* results of n_r at about $\lambda = 1310$ nm agree with those determined *in vivo* from human skin epidermis (averaged over the sc and other sub-layers) by the OCT method (Tearney *et al* 1995, Knuttel and Boehlau-Godau 2000). The n_r of dermis, however, is smaller than the above reported *in vivo* results: 1.36 versus 1.41 at about $\lambda = 1310$ nm. The wavelength dependence is similar to the n_r of bovine and porcine muscle tissues in the visible region (Bolin *et al* 1989, Li and Xie 1996). To extend the use of our real refractive index data on a limited number of wavelengths, we have tested different dispersion schemes based on the equations by Cauchy, Cornu and Conrady. From figures 6 and 7, it is clear that these relations are close to each other and all fit to data fairly well for the dermis and very well for the epidermis. Therefore, these equations may be used to estimate the values of the real refractive indices of human skin tissues with the coefficients given in table 2 between 300 and 1600 nm. These estimations should be further improved as the refractive index becomes available at an increased number of wavelengths in this spectral region.

Acknowledgments

JQL and XHH acknowledge partial support by a NIH grant (1R15GM70798-01). Comments and correspondence should be sent to X H Hu: hux@mail.ecu.edu.

References

- Atchison D A and Smith G 2005 Chromatic dispersions of the ocular media of human eyes *J. Opt. Soc. Am. A Opt. Image Sci. Vis.* **22** 29–37
- Ballenegger V C and Weber T A 1999 The Ewald–Oseen extinction theorem and extinction lengths *Am. J. Phys.* **67** 599–605
- Barrera R G and Garcia-Valenzuela A 2003 Coherent reflectance in a system of random Mie scatterers and its relation to the effective-medium approach *J. Opt. Soc. Am. A Opt. Image Sci. Vis.* **20** 296–311
- Bartlett M A and Jiang H 2001 Effect of refractive index on the measurement of optical properties in turbid media *Appl. Opt.* **40** 1735–41
- Beisson F, Aoubala M, Marull S, Moustacas-Gardies A M, Voultoury R, Verger R and Arondel V 2001 Use of the tape stripping technique for directly quantifying esterase activities in human stratum corneum *Anal. Biochem.* **290** 179–85
- Bohren C F and Huffman D R 1983 *Absorption and Scattering of Light by Small Particles* (New York: Wiley)
- Bolin F P, Preuss L E, Taylor R C and Ference R J 1989 Refractive index of some mammalian tissues using a fiber optic cladding method *Appl. Opt.* **28** 2297–303
- Ding H, Lu J Q, Jacobs K M and Hu X H 2005 Determination of refractive indices of porcine skin tissues and intralipid at eight wavelengths between 325 and 1557 nm *J. Opt. Soc. Am. A* **22** 1151–7
- Duncan A, Meek J H, Clemence M, Elwell C E, Tyszczyk L, Cope M and Delpy D T 1995 Optical pathlength measurements on adult head, calf and forearm and the head of the newborn infant using phase resolved optical spectroscopy *Phys. Med. Biol.* **40** 295–304

- Everett M A, Yeagers E, Sayre R M and Olson R L 1966 Penetration of epidermis by ultraviolet rays *Photochem. Photobiol.* **5** 533–42
- Hale G and Query M 1973 Optical constants of water in the 200 nm to 200 micrometer wavelength region *Appl. Opt.* **12** 555–63
- Knuttel A and Boehlau-Godau M 2000 Spatially confined and temporally resolved refractive index and scattering evaluation in human skin performed with optical coherence tomography *J. Biomed. Opt.* **5** 83–92
- Kroger R H H 1992 Methods to estimate dispersion in vertebrate ocular media *J. Opt. Soc. Am. A Opt. Image Sci. Vis.* **9** 1486–90
- Li H and Xie S 1996 Measurement method of the refractive index of biotissue by total internal reflection *Appl. Opt.* **35** 1793–5
- Lu J Q, Hu X H and Dong K 2000 Modeling of the rough-interface effect on a converging light beam propagating in a skin tissue phantom *Appl. Opt.* **39** 5890–7
- Lu J Q, Yang P and Hu X H 2005 Simulations of light scattering from a biconcave red blood cell using the FDTD method *J. Biomed. Opt.* **10** 024022
- Ma X, Lu J Q, Brock R S, Jacobs K M, Yang P and Hu X H 2003a Determination of complex refractive index of polystyrene microspheres from 370 to 1610 nm *Phys. Med. Biol.* **48** 4165–72
- Ma X, Lu J Q, Ding H and Hu X H 2005 Bulk optical parameters of porcine skin dermis tissues at eight wavelengths from 325 to 1557 nm *Opt. Lett.* **30** 412–4
- Ma X, Lu J Q and Hu X H 2003b Effect of surface roughness on determination of bulk tissue optical parameters *Opt. Lett.* **28** 2204–6
- Meeten G H and North A N 1995 Refractive index measurement of absorbing and turbid fluids by reflection near the critical angle *Meas. Sci. Technol.* **6** 214–21
- Meglinsky I V and Matcher S J 2001 Modelling the sampling volume for skin blood oxygenation measurements *Med. Biol. Eng. Comput.* **39** 44–50
- Tearney G J, Brezinski M E, Southern J F, Bouma B E, Hee M R and Fujimoto J G 1995 Determination of the refractive index of highly scattering human tissue by optical coherence tomography *Opt. Lett.* **20** 2258–60
- Tuchin V V 2005 Optical clearing of tissues and blood using the immersion method *J. Phys. D: Appl. Phys.* **38** 2497–518
- van Gemert M J, Jacques S L, Sterenborg H J and Star W M 1989 Skin optics *IEEE Trans. Biomed. Eng.* **36** 1146–54
- Wang L, Jacques S L and Zheng L 1995 MCML—Monte Carlo modeling of light transport in multi-layered tissues *Comput. Methods Prog. Biomed.* **47** 131–46
- Zhao H, Tanikawa Y, Gao F, Onodera Y, Sassaroli A, Tanaka K and Yamada Y 2002 Maps of optical differential pathlength factor of human adult forehead, somatosensory motor and occipital regions at multi-wavelengths in NIR *Phys. Med. Biol.* **47** 2075–93